J Fluoresc (2013) 23:929–938
DOI 10.1007/s10895-013-1218-6

ORIGINAL PAPER

Sensing of Micellar Microenvironment with Dual Fluorescent Probe, Triazolylpyrene (^{TNDMB}Py)

Subhendu Sekhar Bag · Rajen Kundu

Received: 6 December 2012 / Accepted: 1 April 2013 / Published online: 23 April 2013

Abstract We report a dual fluorescent triazolylpyrene (^{TNDMB}**Py**) as an efficient fluorescent light-up probe of various micellar microenvironments. The absorption spectra of ^{TNDMB}**Py** in an aqueous solution of varying surfactant concentration, CTAB, SDS and TX-100 showed that as the surfactant concentration was increased the absorbance increased with no shift in wavelength maxima. The increase of absorbance in each surfactant solution with increase in surfactant concentration was due to the enhanced solubilization of ^{TNDMB}**Py** in surfactant solutions. Our investigations based on steady state and time resolved fluorescence techniques showed that the probe reports the microenvironment of ionic surfactant solutions (CTAB and SDS) via dual emission (LE and ICT) at low surfactant concentration. The ICT band showed a blue shifting pattern with enhanced intensity that disappeared as the concentration of surfactant increases (> 1 mM for CTAB and > 3 mM for SDS). In non-ionic surfactant (Triton X-100) solution, the fluorophore showed dual emission with dominant ICT behaviour over LE emission at low concentration (up to 0.35 mM). In reverse micelle we observed a blue shifted ICT band with no LE band with increasing molar concentration of water. We found 100 nm blue shifting when we moved from R=0 to R=7, where R is the molar ratio of water to TX-100 (R=[H2O]/[TX-100]). The blue shifting of ICT band is because of the movement of the probe from hydrophilic core to hydrophobic core (surface) of the reverse micelle. Thus from the steady-state fluorescence study it was observed that the ICT band of the probe, ^{TNDMB}**Py** was more influenced by the micellar environment in comparison to the LE band. This difference in behaviour of the fluorophore is probably because of varying extent of hydrophobic/hydrogen bonding interactions experienced by the probe and its relative disposition inside the various micellar nanocores.

Keywords Triazolylpyrene probe · Micelle · Reverse micelle · Micropolarity · LE and ICT emission · Critical micellization concentration (CMC)

Introduction

The study of cell membrane and the role it plays in living cells is necessary to understand cellular function. It is also important to study drug-membrane interaction with a model system which is a real mimic of cell membrane. Micelles are colloidal-sized clusters formed in solutions from the surfactant molecules [1–14]. They are amphiphilic molecules, like lipids, thus, some of the same rules governing lipid behaviour may also apply to the micelle. Therefore, micelles have widely been used as a model of biomembrane to acquire information about structure, microenvironmental properties and function. Micelles play a vital role in both fundamental and applied sciences. Thus, micelles have been used in several applications such as (a) in accommodating and transporting insoluble or sparingly soluble drugs [15], (b) a model of biomembrane because of their similarity in microenvironment to that of proteins, enzymes, phospholipid bilayer and they mimic biomolecular surfaces and properties [16–19], (c) a model of enzyme's catalytic behavior [20, 21]. Many kinds of reverse micelles (consisting of a polar/aqueous inner core and a nonpolar outer surface) [8–14] are able to solubilize fairly large amount of water and hydrophilic molecules, such as proteins. Thus, they

Electronic supplementary material The online version of this article (doi:10.1007/s10895-013-1218-6) contains supplementary material, which is available to authorized users.

S. S. Bag (✉) · R. Kundu
Bioorganic Chemistry Laboratory, Department of Chemistry, Indian Institute of Technology Guwahati, Guwahati 781039, India
e-mail: ssbag75@iitg.ernet.in

found application in biotechnology, in the mimicking of biological structures, in studying the relationship between environment and conformation/activity of functional biopolymers. Many drugs are extremely water-insoluble but may contain many polar moieties. Therefore, a micellar environment that is water insoluble but feature polar groups for dipole interaction or H-bonding can solubilise such drugs thereby micelle can be a carrier of drug candidates.

Therefore, the study of micelles and their role in chemistry, pharmacy, and biology is of paramount importance. Considering the importance of micellar systems in the pharmaceutical field and the many applications that it presents, micelles have widely been used as a model of biomembrane to acquire information about structure, microenvironment properties and functions. Thus, probing of micellar microenvironment with fluorescence sensor molecules or ions is of paramount importance to know the structure and to modulate the charge distribution on the interface and thereby to correlate those with real membrane system. With the introduction of a proper fluorescent probe that is very sensitive to microenvironmental dielectric properties and viscosity, one can study the process of micellisation and also the effect of interfacial electric field on the probe thereby enabling correlation with the biomembrane. In the past few decades considerable efforts have been devoted to investigate the structure, functions, and biological applications of the micelle. Among the various methods available, fluorescent based technique by using a suitable environment sensitive fluorescent probe is one of the most important, easier and efficient technique to determine the structure of micelle and its function. Fluorescence properties of a polarity sensitive probe are highly sensitive towards its surrounding environments. Thus, when a probe comes in contact with surfactant molecules, its emission intensity may either be enhanced or decreased and/or the position of emission wavelength (λ^{fl}_{max}) may be shifted from its original band position either to a shorter or to a longer wavelength region. Among the various fluorescent probes, charge transfer fluorescent probes being by far the most polarity sensitive probes are very important and efficient to probe micellar microenvironment, thereby enabling the determination of structure and function of micelle via the generation of a distinct fluorescence signal.

A substantial amount of research have been carried out to understand the photophysics and the photochemistry of fluorescent molecules in micellar solution [22–28]. Incorporation of the molecular probe into the aqueous micelles effectively reveals parameter such as CMC, roughness of the micelle surfaces, polarity, viscosity and degree of water penetration into these surfactant aggregations. Most of the probes have been chosen for their particular affinity for one or two of the principal micellar region: the hydrocarbon core formed from surfactants tails, the interface composed primarily of the amphiphilic head groups, or surrounding aqueous solvent phase. Many of the probes are soluble in an extensive range of media, suggesting their inability of probing of specific micellar domains [4, 5, 29, 30]. There are limited numbers of fluorophore that can selectively target specific micellar domains [31]. Therefore, there is need for development of probes with specificity of probing micellar microenvironment via the generation of enhanced fluorescence signal.

As a part of our ongoing search for a suitable environmentally sensitive fluorescent probe, we recently have developed triazolylpyrene (^{TNDMB}**Py**) as a dual fluorescent probe [32]. Our ongoing observations on fluorescence switch-on probing of ct-DNA, BSA and Cu^{2+} ion led us to explore the possibility of utilising our designed "smart" dual-fluorescent probe, triazolylpyrene (^{TNDMB}**Py**) in probing of micellar microenvironment. We envisaged that formation of self-assembled complex with the micelle would result in a significant change in the fluorescence emission intensity of either of the LE band (monomer band) or the ICT band or both of the bands of triazolylpyrene. Thus, sensing micellar microenvironment can be achieved by evaluating spectral characterisctics of our probe. Keeping this view in our mind, we have framed our objective as follow: (a) to investigate the photophysical property of triazolylpyrene (^{TNDMB}**Py**), in presence of various surfactants (cationic, anionic and non-ionic) of varying concentration. (b) As we know that, the reverse micelle system is a real mimic of cell membrane, we, thus also interested in studying the photophysical properties of ^{TNDMB}**Py** in reverse micelle of TX-100 in benzene-hexane (3:7) and water system.

Results and Discussions

Study of Photophysical Properties

The synthesis of the probe (^{TNDMB}**Py)** was achieved following our reported click chemistry protocol with very high yield [32]. After characterizing and recrystallization which afforded very pure compound we then turned our attention to study the photophysical properties of the probe in various media. Previously we have reported in detailed the photophysical properties of triazolylpyrene in presence of various solvents and solvent mixtures with varying dielectric constant. In a summary the absorption spectrum of the probe did not markedly differ with the solvent polarity; however the emission spectrum strongly differed with the solvent polarity. The molecule showed a dual emission behavior centered at 383 nm, a locally emission (LE) band and 466–544 nm, internal charge transfer (ICT) band (Fig. 1). In high polar solvents (acetonitrile, methanol) the probe showed a low intense LE (local emission) band, characteristic structured band of pyrene. In ether, dioxane, toluene, chloroform and ethyl acetate a dual emission was

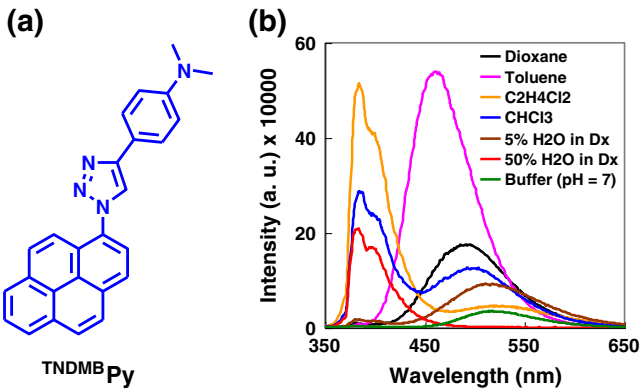

Fig. 1 **a** Structure of triazolylpyrene probe and **b** emissions behavior of the probe in different solvents

observed along with a strong red shifted pattern of the ICT (internal charge transfer) band as the solvent polarity increased from toluene (466 nm) to ethyl acetate (544 nm) [32]. Our probe consists of a *N,N*-dimethyl aminophenyl donor linked triazole functional which serves as an efficient electron donor and a pyrene functional which acts as an electron acceptor. Thus, the probe consists of an efficient charge transfer property. A dioxane water titration revealed that the long wavelength emission band is not because of aggregation (see Supplementary data). Linear increasing relationship between absorbance and emissions at both the emission wavelengths and concentration of the probe suggested that the long wavelength emission band originated purely from an intermolecular charge transfer (ICT) state and not because of excimer emission (see Supplementary data).

Study of UV-Visible Spectra

Next, we have studied, the photophysical properties of probe in presence of cationic (CTAB), anionic (SDS) and non-ionic (Triton X-100) surfactant and in presence of reverse micelle (TX-100 in 3:7 benzene-hexane and water system). Thus, the absorption spectra of ^{TNDMB}**Py** in aqueous solutions of varying surfactant concentration, CTAB, SDS (Fig. 2) and TX-100 and in reverse micelle (Fig. 3) were recorded keeping the concentration of the probe fixed. From these spectra it is clear that the absorbance of the probe is increased with increase in surfactant concentrations even beyond the critical micellization concentrations of all the surfactants. However, the absorption wavelength maxima, λ_{max}^{abs} remains unaltered and centered at around 344 nm in all the cases. The increase in absorbance in each surfactant solution with increase in surfactant concentration is attributed to the enhanced solubilization of the probe (^{TNDMB}**Py**) in surfactant solutions.

However, in reverse micellar system we observed no regular change in absorbance value, with increase in molar ratio of water.

Study of Fluorescence Spectra

The steady state fluorescence techniques have been widely used to study the miceller microenvironment and the mechanism of micelle formation with the help of a suitable fluorescent probe. As our designed probe, ^{TNDMB}**Py** consists of a donor (*N,N*-dimethyl aminophenyl linked with triazole) as well as acceptor (pyrene) groups linked via a triazole unit, so there may be a possibility of charge transfer in the excited state, which would be affected by the polarity of the surrounding environment. The charge transfer phenomenon of the probe, ^{TNDMB}**Py** in dioxane-water system was well studied. A dual fluorescence emission (LE, local emission and ICT, internal charge transfer) was observed in dioxane-water solvent system. With increase of % of water content, a red shifted ICT band with decreased intensity was observed. It was studied that the dual fluorescence appears from the equilibrium between two states, LE and ICT in the excited state [32]. The short wavelength emission band arises from the locally excited (LE) state and the long

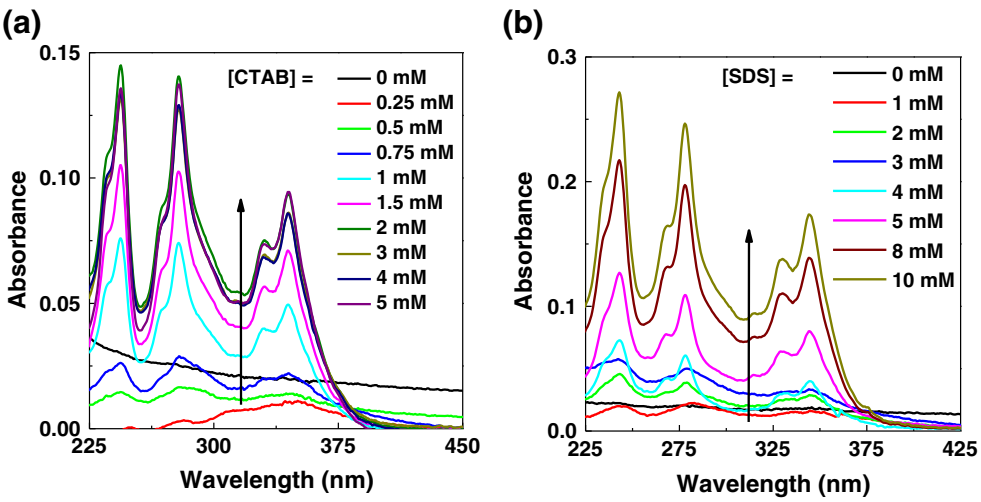

Fig. 2 UV-visible spectra of ^{TNDMB}**Py** in aqueous solution of varying surfactant concentration of (**a**) CTAB and (**b**) SDS. [^{TNDMB}**Py**]=10 μM

wavelength emission band arises from the newly generated ICT state having higher dipole moment than the LE state. The ICT state is stabilized by the solvent polarity and thus the energy gap between ground and excited state decreases and we observe a long wavelength emission, called ICT band.

The steady-state fluorescence spectra of ^{TNDMB}**Py** in all three surfactant solutions, CTAB, SDS and TX-100 as well as in reverse micelle were recorded. In ionic surfactant solution a dual emission (LE and ICT) was observed at low surfactant concentration (insets Fig. 4). The ICT band showed a blue shifting pattern with enhanced intensity that disappeared as the concentration of surfactant increases (> 1 mM for CTAB and > 3 mM for SDS, Fig. 4a and b respectively). Thus, this observation suggested that micro-environment around the probe, ^{TNDMB}**Py** is different from the pure aqueous phase. The spectral shifts and the enhancement of the fluorescence intensities of ICT band at low surfactant concentration and gradual increase of the fluorescence intensities of LE band with the increase in surfactant concentration can be explained in terms of binding of this probe to a less polar site of the micelle.

In nonionic surfactant solution, Triton X-100 and in reverse micelle of Triton X-100 in benzene-hexane and water system, we observed an interesting emission behavior of the probe ^{TNDMB}**Py**. Thus, in low TX-100 concentration (up to 0.35 mM), the fluorophore showed dual emission with dominant ICT emission over LE emission. However, at high concentration the LE band predominates over ICT band (Fig. 5a).

In reverse micelle we observed a blue shifted patter of the ICT band with no emission from LE state as the molar concentration of water is increased (Fig. 5b). We found 100 nm blue shifting when we moved from R=0 to R=7, where R is the molar ratio of water to TX-100 (R=[H2O]/[TX-100]). The blue shifting of ICT band is probably because of movement of the probe from hydrophilic core to more hydrophobic core (surface) of the reverse micelle. Thus, from the steady-state fluorescence study it was observed that the ICT band of the probe, ^{TNDMB}**Py** was more influenced by the micellar environment in comparison to the LE band.

Time Resolved Fluorescence Study

Fluorescence lifetime of a molecule is very sensitive towards its local environment. Thus this study can nicely explain the location and distribution of the probe in micellar microenvironment. The time resolved fluorescence spectra of ^{TNDMB}**Py** were recorded in all three surfactant solutions, CTAB (Fig. 4c), SDS (Fig. 4d) and TX-100 (Fig. 5c) as well as in reverse micelle of Triton X-100 in benzene-hexane and water system (Fig. 5d).

The fluorescent life time (τ) was expressed using the following two equations.

$$a_n = \frac{B_n}{\sum_{i=1}^{N} B_i} \tag{1}$$

where a is the fluorescence lifetime coefficient and B is the pre-exponential factor. The mean lifetime was calculated by the following equation

$$\langle \tau \rangle = \frac{\sum a_i \tau_i^2}{\sum a_i \tau_i} \tag{2}$$

where τ_i and a_i are the fluorescence lifetime and its coefficient of the i^{th} component respectively

From the time resolved fluorescence study, it was observed that the decay time (τ) of ^{TNDMB}**Py** increases with increasing surfactant concentration for all three surfactants (CTAB, SDS and TX-100). These results showed a good correlation with the steady state fluorescence study, where we observed an increase in fluorescence intensity with increase in surfactant concentration. In SDS surfactant, a bi-exponential decay with increasing mean lifetime (<τ>) of ^{TNDMB}**Py** was observed as the concentration of SDS was increased (Table 1 and Fig. 4d).

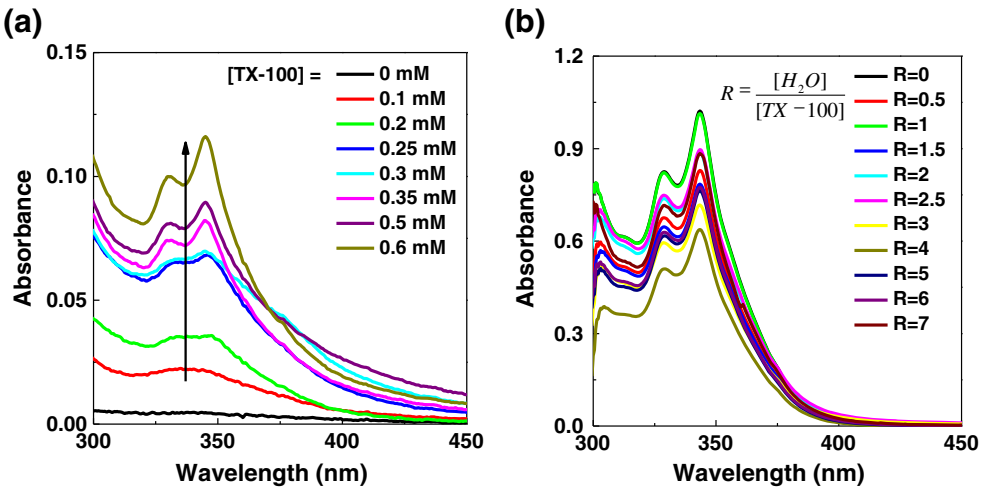

Fig. 3 UV-visible spectra of ^{TNDMB}**Py** in **a** aqueous solution of varying TX-100 concentration and **b** in reverse micelle of TX-100 in benzene-hexane (3:7) and water mixture. [^{TNDMB}**Py**]=10 μM

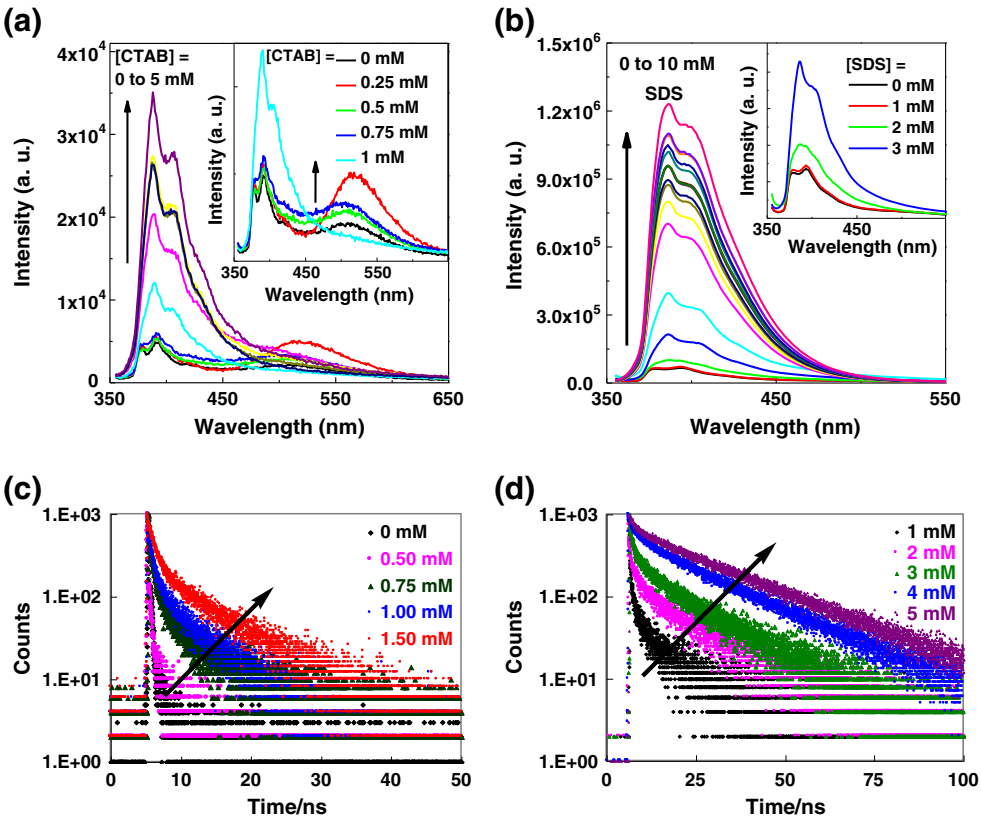

Fig. 4 Fluorescence spectra (λ_{ex}=343 nm) of ^{TNDMB}**Py** in aqueous solution of varying surfactant concentration of **a** CTAB and **b** SDS. [^{TNDMB}**Py**]=10 μM. Time resolved fluorescence spectra of ^{TNDMB}**Py** in presence of **c** CTAB and **d** SDS (λ_{em}=LE band)

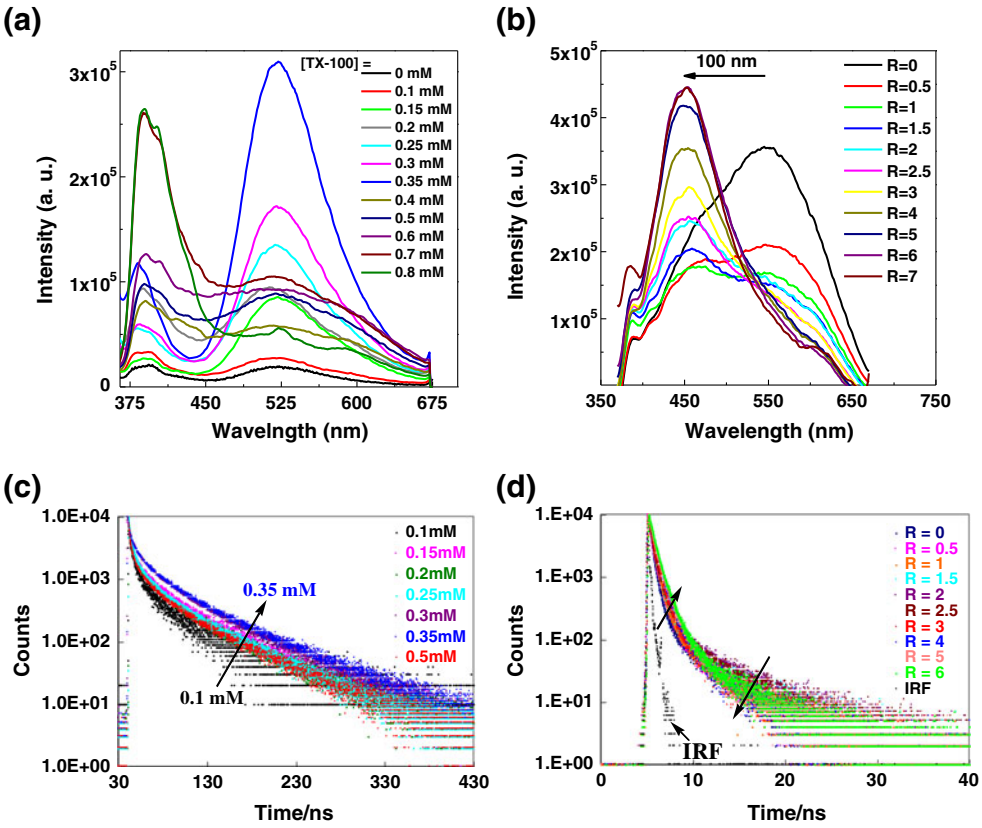

Fig. 5 Fluorescence spectra (λ_{ex}=343 nm) of ^{TNDMB}**Py** **a** in aqueous solution of varying concentration of TX-100 surfactant and **b** in reverse micelle of TX-100 in benzene-hexane (3:7) and water mixture. R is molar ratio of water to TX-100. Time resolved fluorescence spectra of ^{TNDMB}**Py** in presence of **c** TX-100 surfactant and **d** in reverse micelle of TX-100 (λ_{em}=ICT band)

Table 1 Summary of time resolved fluorescence of ^{TNDMB}**Py** in presence of SDS, monitored at LE band (400 nm)

[SDS] (mM)	τ_1 (ns)	τ_2 (ns)	<τ> (ns)	Amplitude	
				B_1	B_2
1	0.74 (77.3 %)	8.54 (22.7 %)	6.76	91.04	26.69
2	2.07 (60.8 %)	16.7 (39.2 %)	14.3	91.28	58.78
3	2.10 (53.1 %)	16.5 (46.9 %)	14.7	132.40	116.84
4	2.68 (37.5 %)	21.5 (62.5 %)	20.2	294.59	491.77
5	2.23 (27.1 %)	24.7 (72.9 %)	24.0	236.13	633.78

The mean lifetime increases from 6.76 ns in 1 mM SDS to 24.0 ns in 5 mM SDS concentration. The increase in decay time and the fluorescence intensity is probably because of substantial decrease in non-radiative decay in the micellar environment. From the bi-exponential fitting we observed that τ_1 and τ_2 increases (monitoring wavelength was LE band) with increasing surfactant concentration, however, the abundance of first component (a_1) decreases and the second component (a_2) increases with increasing surfactant concentration.

Time resolved fluorescence was also measured by monitoring the ICT band (515–480 nm) in SDS surfactant solution (Table 2 and see Supplementary data). A bi-exponential fitting of the decay curve revealed that as SDS concentration increases from 1 mM to 3 mM, the mean lifetime decreases. This result also correlates well with the steady state fluorescence study, where we observed no ICT band at high SDS (> 3 mM) concentration.

Next, we have measured the lifetime of the probe in presence of cationic surfactant, CTAB solution (Fig. 4c). The lifetime data were fitted to a biexponential decay fitting curve. Thus, similar to the case of SDS surfactant, a bi-exponential decay with increasing mean lifetime (<τ>) of ^{TNDMB}**Py** was observed as the concentration of CTAB was increased (Table 3 and Fig. 4c). The mean lifetime increases from 0.53 ns in water to 6.41 ns in 1.5 mM CTAB concentration. The increase in decay time and the fluorescence intensity is probably because of substantial decrease of non-radiative decay in the micellar environment.

After measuring the time resolved fluorescence of the probe in presence of ionic surfactants we next investigated the same in presence of neutral surfactant. Thus, we observed a similar result in presence of non-ionic surfactant as that was observed in the case of ionic surfactant. The decay time of ^{TNDMB}**Py** was increased with increase in concentration of TX-100 up to 0.35 mM, and then it started decreasing as the concentration was increased beyond 0.35 mM (Fig. 5c, Table 4). Our result on the time resolved fluorescence response of the probe upon changing the concentration of neutral surfactant showed a very good correlation with the steady state fluorescence study where an increase in intensity was observed till the concentration of TX-100 increased to 0.35 mM and it decreased upon further increase in concentration of TX-100. We observed a bi-exponential fitting with increase in mean decay time from 28.1 ns in 0.1 mM TX-100 to 50.7 ns in 0.35 mM TX-100. Further increase in concentration of TX-100 showed a decrease in decay time of the probe (45.1 ns in 0.5 mM TX-100, Fig. 5c, Table 4).

After studying the photophysical behaviours of the probe in anionic, cationic and neutral surfactant solution, we next turn our attention to study the time resolved fluorescence behaviour of our probe in presence of TX-100 in benzene-hexane-water system where reverse micelle formation takes place. Thus, we observed a multi exponential fitting with slight change in the decay time in this reverse micellar system (Fig. 5d and Table 5).

Thus, a triexponential decay fitting with very short decay time of the first two major components and a long decay time (τ_3=4.35 ns) with least abundant (1.64 %) third component was observed when R=0. The decay time of the third component increases from 4.35 ns to 5.73 ns upon increase in R=0 to R=2.5 and beyond R=2.5, it decreased. However, the decay time of first two components showed gradual increase with increase in molar ratio of water (Table 5).

Table 2 Time resolved fluorescence summary of ^{TNDMB}**Py** in presence of SDS monitored at ICT band

[SDS] (mM)	$\lambda_{em(ICT)}$ (nm)	τ_1 (ns)	τ_2 (ns)	<τ> (ns)	Amplitude	
					B_1	B_2
1	515	4.2 (60.46 %)	25.34 (39.54 %)	21.07	122.44	80.07
2	500	3.26 (64.64 %)	19.22 (35.36 %)	15.44	80.75	44.17
3	480	2.57 (70.95 %)	19.85 (29.05 %)	15.70	95.51	39.10

Table 3 Time resolved fluorescence summary of ^{TNDMB}**Py** in presence of CTAB, monitored at LE band (400 nm)

[CTAB] (mM)	τ_1 (ns)	τ_2 (ns)	<τ> (ns)	Amplitude	
				B_1	B_2
0	0.24 (90.8 %)	1.15 (9.2 %)	0.53	132.18	13.36
0.5	0.35 (93.5 %)	1.97 (6.5 %)	0.80	80.49	5.62
0.75	0.80 (78.7 %)	5.93 (21.3 %)	4.22	129.87	35.19
1	0.86 (74.9 %)	6.56 (25.1 %)	4.94	154.71	51.79
1.5	0.99 (70.2 %)	7.99 (29.8 %)	6.41	238.23	101.16

Determination of Critical Micellization Concentration (CMC)

Surfactant molecules aggregate in liquid to form micelle in solution. At which concentration, the surfactant molecules formed micelles is called the critical micelle concentration (CMC). The microenvironments above and below the CMC are different. From the steady-state fluorescence study we observed that the fluorescence intensity of the probe, ^{TNDMB}**Py** increases with increase in surfactant concentration for the case of all surfactant solution (SDS, CTAB and TX-100). After a certain concentration limit the fluorescence intensity drastically jumped to a higher value and again smoothly increases. Thus, the CMC value of all the three surfactants, CTAB, SDS and TX-100 were calculated with the help of steady-state fluorescence spectra of ^{TNDMB}**Py**. The plots of fluorescence Intensity vs. [surfactant] are shown in the following Fig. 6. The experimental CMC values of three surfactants obtained from the plots were 0.7 mM for CTAB, 6.5 mM for SDS and 0.26 mM for TX-100 are close and comparable with the literature reported values of 0.94 mM for CTAB, 7.80 mM for SDS and 0.26 mM for TX-100 (Table 6).

Determination of Binding Constant

The fluorescence intensity of the probe in aqueous and in micellar media is far different. Thus, the binding constant (K) of the probe with micelle was calculated from the fluorescence intensity values in micelle media. We used the following relationship demonstrated by Almgren et al., [34] to calculate the binding constants (Ks) of the probe in various micelles.

$$\frac{(I_\infty - I_0)}{(I_t - I_0)} = 1 + (K[M])^{-1} \tag{3}$$

where I_∞, I_0, and I_t are the fluorescence intensities of the probe under complete micellization, in the absence of micellization, and in presence of intermediate amounts of surfactant, respectively. [M] is the micelle concentration, which can be expressed by the following relationship

$$[M] = \frac{(S - CMC)}{N} \tag{4}$$

where S is the surfactant concentration, CMC is the critical micelle concentration and N is the aggregation number of the micelle. The N values used in the calculation of [M] are 60 for CTAB, 62 for SDS, and 143 for Triton X-100 [35]. The plots of $(I_\infty - I_0)/(I_t - I_0)$ vs. $[M]^{-1}$ for all the three micelles, CTAB, SDS and TX-100 are shown in Fig. 7a-c respectively.

The calculated binding constants of the probe in various micelles are summarized in Table 6. Thus, we have seen that the binding constant of the probe with

Table 4 Time resolved fluorescence summary of ^{TNDMB}**Py** in presence of TX-100, monitored at ICT band (520 nm)

[TX-100] (mM)	τ_1 (ns)	τ_2 (ns)	<τ> (ns)	Amplitude	
				B_1	B_2
0.1	4.02 (84.9 %)	41.3 (15.1 %)	28.1	572.23	101.50
0.15	10.6 (64.7 %)	56.2 (35.3 %)	44.5	1981.66	1082.10
0.2	10.2 (67.3 %)	54.1 (32.7 %)	41.8	1870.381	910.27
0.25	11.0 (68.4 %)	57.2 (31.6 %)	43.6	1924.27	889.86
0.3	11.7 (63.8 %)	57.5 (36.2 %)	45.4	2689.36	1525.56
0.35	15.0 (62.5 %)	64.5 (37.5 %)	50.7	2159.30	1293.09
0.4	13.6 (55.5 %)	60.0 (44.5 %)	49.8	2545.23	2037.48
0.5	11.6 (63.1 %)	56.9 (36.9 %)	45.1	1292.52	756.16
0.7	8.95 (70.5 %)	51.1 (29.5 %)	38.7	1002.11	419.59

Table 5 Time resolved fluorescence summary of ^{TNDMB}**Py** in presence of reverse micelle, monitored at ICT band

R[a]	λ_{em} (nm)	τ_1 (ns)	τ_2 (ns)	τ_3 (ns)	<τ> (ns)	Amplitude		
						B_1	B_2	B_3
0	460	0.266 (72.81 %)	0.700 (25.55 %)	4.35 (1.64 %)	1.10	7054.78	2476.22	158.88
0.5	460	0.269 (60.66 %)	0.766 (37.86 %)	4.50 (1.48 %)	1.09	5937.20	3705.49	144.51
1	460	0.276 (61.20 %)	0.764 (37.25 %)	4.57 (1.56 %)	1.12	5898.99	3590.56	150.09
1.5	455	0.298 (61.10 %)	0.820 (37.32 %)	5.15 (1.57 %)	1.27	5874.53	3588.46	151.12
2	450	0.339 (66.16 %)	0.912 (32.09 %)	5.64 (1.75 %)	1.46	6193.60	3004.39	163.75
2.5	450	0.366 (68.98 %)	0.955 (29.54 %)	5.73 (1.49 %)	1.37	6420.28	2749.14	138.62
3	450	0.384 (63.86 %)	0.909 (35.08 %)	5.18 (1.06 %)	1.08	5937.21	3260.93	98.41
4	450	0.474 (66.95 %)	1.02 (31.93 %)	4.96 (1.12 %)	1.09	6327.04	3017.93	106.00
5	450	0.485 (63.89 %)	1.05 (36.06 %)	5.11 (0.05 %)	0.81	6019.18	3397.44	4.59
6	450	0.502 (61.91 %)	1.07 (37.02 %)	5.28 (1.07 %)	1.15	6005.99	3590.79	104.03

[a] R = $[H_2O]/[TX\text{-}100]$

cationic, anionic and non-ionic micelle follow the order CTAB<SDS<TX-100.

The excited state dipole moment of triazolylpyrene was calculated to be 17.07 D [32]. During the course of charge transfer process from the donor *N,N*-dimethylaminophenyltriazol unit to the acceptor pyrene of the probe, the $-NMe_2$ group will carry more positive charge and the acceptor part will carry more negative charge. In case of SDS micelle the Stern layer contains negatively charged head groups and the Gouy-Chapman layer contains positively charged counter ions. Therefore, the probe more likely would reside in the hydrophobic core of the micelle exposing toward Stern layer. This is supported by quenching of monomer emission of the probe by Cu^{2+} as quencher in the SDS micellar environment [36]. In aqueous medium of SDS solution the probe showed only a local emission at around 390 nm with no ICT emission. Upon addition of Cu^{2+} ion a fluorescence quenching of the LE band was observed [36]. This can be explained if we consider an electron transfer process from the pyrene unit to the Cu^{2+} ion in micelle-probe interface.

Conclusions

In conclusion, we have investigated the photophysical response of a donor acceptor charge transfer fluorescent probe, triazolylpyrene (^{TNDMB}**Py)** inside the micellar microenvironment. In ionic surfactant solution the probe showed a dual emission (LE and ICT) at low surfactant concentration. The ICT band showed a blue shifting pattern with enhanced intensity that disappeared as the concentration of surfactant increases (> 1 mM for CTAB and > 3 mM for SDS). At low concentration of non-ionic surfactant TX-100, the probe showed dual emission with dominant ICT emission over LE emission. However, at high concentration of TX-100, the LE band predominates over ICT band. In reverse micelle a blue shifted pattern of the ICT band with no LE band was observed with increase in molar concentration of water. Over all, the

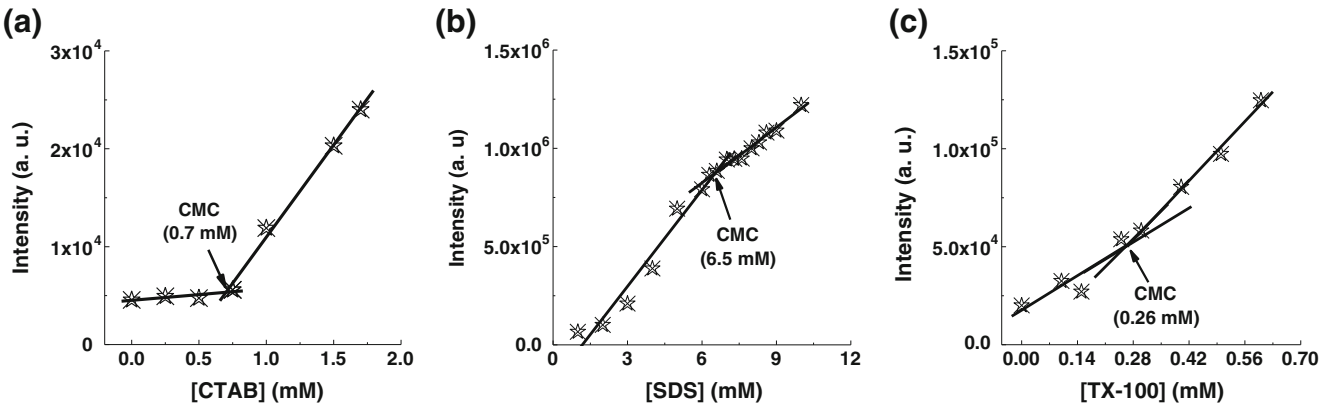

Fig. 6 Plots of fluorescence intensity vs. **a** [CTAB], **b** [SDS] and **c** [TX-100]

Table 6 Summary table for the CMC and binding constant values

Medium	CMC (mM) (Experimental)	CMC (mM) (Reported) [33]	Binding Constant (K_{eq}) (M^{-1})
CTAB	0.70	0.94	4.28×10^4
SDS	6.50	7.80	2.12×10^5
TX-100	0.26	0.26	6.84×10^5

ICT emission was found to be modulated much more by the media than the LE emission. The changes in polarity and strong interaction of the probe with micelles deactivate the non-radiative decay channels thereby increasing fluorescence intensity. The micelle probe interaction was studied spectroscopically. The experimental CMC values of surfactant from the fluorescence intensity vs. [surfactant] plot are in good agreement with the literature reported values. The binding constant of the probe with cationic, anionic and non-ionic micelle follow the order CTAB<SDS<TX-100. Thus, we have successfully demonstrated that our probe, triazolylpyrene (^{TNDMB}**Py**) is an efficient fluorescence switch-on probe of micellar microenvironment. Therefore, our probe might find application in probing of membrane in biological systems which expectedly would generate a distinct fluorescence signal for such interaction events and shed light to the environment around it inside the cell.

Materials and Methods

Materials

CTAB, SDS, benzene and hexane were purchased from Merck, India. Triton X-100 was purchased from SRL, India. Water was obtained from a Milli-Q purification system. All experiments were performed with freshly prepared solutions in Milli-Q water. The probe molecule was synthesized and purified according to the reported procedure. We recrystallised the column purified material in choloform-ethylacetate solvent mixture twice, dried under vacuum, again characterized and used for study.

Preparation of Probe-Surfactant Solutions

The various concentrations of a particular surfactant solution were prepared by using Milli-Q water. Then the surfactant solutions of various concentrations were added to the sample vials containing probe. The sample solutions were mixed well before the experiment.

UV–Visible Study

The UV–Visible absorbance measurements were performed using Shimadzu 2550 UV/vis spectrophotometer with a cell of 1 cm path length at 298 K. The probe with surfactant solutions were mixed well before doing the experiment. The measurements were taken in absorbance mode. The absorbance values of the sample solutions were measured in the wavelength regime of 200–600 nm.

Fluorescence Study

All fluorescence studies were performed using a Fluoromax 4 spectrophotometer with a cell of 1 cm path length at room temperature. The excitation wavelength for probe (^{TNDMB}**Py**) was set at 343 nm, and emission spectra were measured in the wavelength regime of 350–675 nm. The probe with surfactant solutions were mixed well before doing the experiment. Fluorescence lifetimes were measured by Edinburgh instrument, Life Space II with Edinburgh 375 nm Laser source for excitation. The fluorescence decay was analyzed by tail fitting method using in built software. All the experiments were carried out at 298 K.

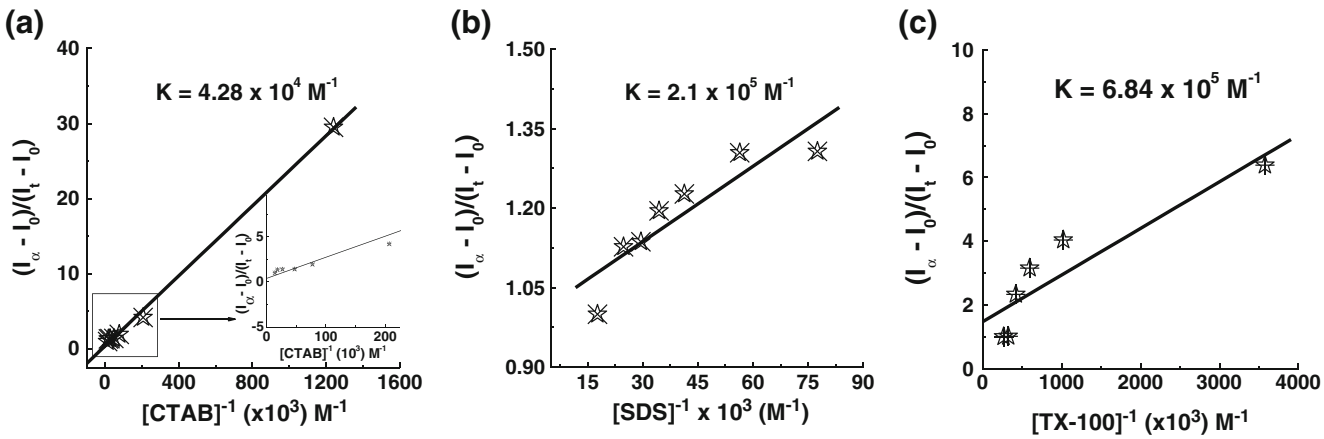

Fig. 7 Plots of $(I_\infty - I_0)/(I_t - I_0)$ vs. [Surfactant]$^{-1}$ of ^{TNDMB}**Py** for **a** CTAB, **b** SDS and **c** TX-100

Acknowledgments Authors thank Department of Science and Technology [DST: SR/SI/OC-69/2008], Govt. of India, for a financial support. R. K. thanks IIT Guwahati, India, for a fellowship.

References

1. Paradies HH (1980) Shape and size of a nonionic surfactant micelle. Triton X-100 in aqueous solution. J Phys Chem 84:599–607
2. Attwood D, Florence AT (1983) Surfactant Systems; Chapman Hall: London
3. Lang J and Zana R (1987) Surfactant solutions: New methods of investigation, In Zana R (Ed.), Surfactant science series, Vol. 22, Marcel Dekker, New York, Chapter 8, pp. 405–4.52
4. Gehlan M, DeSchryver FC (1993) Time-resolved fluorescence quenching in micellar assemblies. Chem Rev 93:199–221
5. Kalyansundaram K (1987) Microheterogeneous systems. Academic, New York
6. Phillies GDJ, Hunt RH, Strang K, Sushkin N (1995) Aggregation number and hydrodynamic hydration levels of Brij-35 micelles from optical probe studies. Langmuir 11:3408–3416
7. Phillies GDJ, Yambert JE (1996) Solvent and solute effects on hydration and aggregation numbers of triton X-100 micelles. Langmuir 12:3431–3436
8. Laughlin RG (1994) The aqueous phase behavior of surfactants. Academic, London
9. Guharay J, Sengupta PK (1996) Characterization of the fluorescence emission properties of 7-Azatryptophan in reverse micellar environments. Biochem Biophys Res Commun 219:388–392
10. Zachariasse KA, Yoshihara T, Druzhinin SI (2002) Picosecond and nanosecond fluorescence decays of 4-(Dimethylamino) phenylacetylene in comparison with those of 4-(Dimethylamino) benzonitrile. No evidence for intramolecular charge transfer and a nonfluorescing intramolecular charge-transfer state. J Phys Chem A 106:6325–6333
11. Bhattacharyya K (2003) Solvation dynamics and proton transfer in supramolecular assemblies. Acc Chem Res 36:95–101
12. Shaw AK, Pal SK (2007) Fluorescence relaxation dynamics of acridine orange in Nanosized micellar systems and DNA. J Phys Chem B 111:4189–4199
13. Sedgwick MA, Crans DC, Levinger NE (2009) What is inside a nonionic reverse micelle? Probing the interior of igepal reverse micelles using decavanadate. Langmuir 25:5496–5503
14. Rafiq S, Yadav R, Sen P (2010) Microviscosity inside a nanocavity: a femtosecond fluorescence up-conversion study of malachite green. J Phys Chem B 114:13988–13994
15. Mall S, Buckton G, Rawlins DA (1996) Dissolution behaviour of sulphonamides into sodium dodecyl sulfate micelles: a thermodynamic approach. J Pharm Sci 85:75–78
16. Caetano W, Tabak M (1999) Interaction of chlorpromazine and trifluoperazine with ionic micelles: electronic absorption spectroscopy studies. Spectrochim Acta Part A: Molecular and Biomolecular Spectroscopy 55:2513–2528
17. Yushmanov VE, Perussi JR, Imasato AC, Rugiero M, Tabak M (1994) Ionization and binding equilibria of papaverine in ionic micelles studied by 1H NMR and optical absorption spectroscopy. Biophys Chem 52:157–163
18. Fresta M, Guccione S, Beccari AR, Furneri PM, Puglisi G (2002) Combining molecular modeling with experimental methodologies: mechanism of membrane permeation and accumulation of ofloxacin. Bioorg Med Chem 10:3871–3889
19. Israelachvili JN (1991) Intermolecular and surface forces, 2nd edn. Academic, London
20. Price SE, Jappar D, Lorenzo P, Saavedra JE, Hrabie JA, Davies KM (2003) Micellar catalysis of nitric oxide dissociation from Diazeniumdiolates. Langmuir 19:2096–2102
21. Rosen MJ (1989) Surfactants and interfacial phenomena, 2nd edn. John Wiley & Sons, New York
22. Sarkar A, Pramanik S, Banerjee P, Bhattacharya SC (2008) Interaction of 1-anthracene sulphonate with cationic micelles of alkyl trimethyl ammonium bromides (CnTAB): A spectroscopic study. Colloids Surf A Physicochemical and Engineering Aspects 317:585–591
23. Ali M, Jha M, Das SK, Saha SK (2009) Hydrogen-Bond-Induced microstructural transition of ionic micelles in the presence of neutral naphthols: pH dependent morphology and location of surface activity. J Phys Chem B 113:15563–15571
24. Banerjee P, Pramanik S, Sarkar A, Bhattacharya SC (2008) Modulated Photophysics of 3-Pyrazolyl-2-pyrazoline derivative entrapped in micellar assembly. J Phys Chem B 112:7211–7219
25. Chakrabarty A, Das P, Mallick A, Chattopadhyay N (2008) Effect of surfactant chain length on the binding interaction of a biological photosensitizer with cationic micelles. J Phys Chem B 112:3684–3692
26. Lopez F, Cuomo F, Ceglie A, Ambrosone L, Palazzo G (2008) Quenching and dequenching of pyrene fluorescence by nucleotide monophosphates in cationic micelles. J Phys Chem B 112:7338–7344
27. Fuguet E, Ràfols C, Bosch E, Rosés M (2003) Characterization of the solvation properties of sodium *n*-Dodecyl sulfate micelles in buffered and unbuffered aqueous phases by solvatochromic indicators. Langmuir 19:55–62
28. Biver T, Boggioni A, Secco F, Venturini M (2008) Gallium(III)/4-(2-Pyridylazo)resorcinol system in water and SDS solution: kinetics and thermodynamics. Langmuir 24:36–42
29. Almgren M (1992) Diffusion-influenced deactivation processes in the study of surfactant aggregates. Adv Colloid Interface Sci 41:9–32
30. Karuskstis KK, Suljak SW, Waller PJ, Whiles JA, Thompson EHZ (1996) Fluorescence analysis of single and mixed micelle systems of SDS and DTAB. J Phys Chem 100:11125–11132
31. Bandyopadhyay P, Ghosh AK, Bandyopadhyay S (2009) Brij-micelle and polyacrylic acid interaction investigated by Cu2+-induced pyrene fluorescence: effect of brij-micelle structure. Chem Phys Lett 476:244–248
32. Bag SS, Kundu R (2011) Installation/Modulation of the emission response via click reaction. J Org Chem 76:3348–3356
33. Kalyanasundram K (1987) Photochemistry in microheterogeneous systems. Academic, New York
34. Almgren M, Griesser F, Thomas JK (1979) Dynamic and static aspects of solubilization of neutral arenes in ionic micellar solutions. J Am Chem Soc 101:279–291
35. Saroja G, Ramachandram B, Saha S, Samanta A (1999) The fluorescence response of a structurally modified 4-Aminophthalimide derivative covalently attached to a fatty acid in homogeneous and micellar environments. J Phys Chem B 103:2906–2911
36. Bag SS, Kundu R, Talukdar S (2012) Fluorometric sensing of Cu^{2+} ion with smart fluorescence light-up probe, triazolylpyrene (^{TNDMB}Py). Tetrahedron Lett 53:5875–5879